Research Article

Antimicrobial, Haemolytic and Antibiofilm Assay of Green Synthesized Silver Nanoparticles by Aqueous Extracts of *Rubia cordifolia*

Surendra Doddarasinakere Mariswamy[1], Chandrashekar Kagepura Thimmaiah [2], Vasantha Kumar Basappachidananda[3], Mahesh Basavaraju[4], Chamaraja Nelligere Arkeswaraiah[4]*

[1]Department of Chemistry, Viday Vikas Institute of Engineering and Technology, (Affiliated to Visvesvaraya Technological University, Belagavi, Karnataka), Mysuru, Karnataka, India.

[2]Institute of Excellence, Vijnana Bhavan, University of Mysore, Mysuru, Karnataka, India.

[3]Department of Chemistry (PG) Sarada Vilas college, Krishnamurthypurm, Mysuru, Karnataka, India.

[4]Department of Chemistry, JSS Academy of Technical Education (Affiliated to Visvesvaraya Technological University, Belagavi, Karnataka), Bengaluru, Karnataka, India.

***Corresponding author's E-mail:** chamarajchem@gmail.com

Received: 16-02-2021; **Revised:** 24-03-2021; **Accepted:** 30-03-2021; **Published on:** 20-04-2021.

ABSTRACT

In the present investigation, a simple and effective green synthesis of silver nanoparticles uncoiled by using root and stem extracts from *Rubia cordifolia* (RC) followed by characterization and evaluation of their in-vitro antibacterial activity against human pathogenic bacterias. The biosynthesized silver nanoparticles had evaluated by using diverse physicochemical methods such as UV-Vis, XRD, DLS, FTIR, SEM, and EDS. These AgNPs showed an absorption peak in the range of 230-292 nm. AgNPs embraced a hexagonal or nearly spherical shape and the dimension of 105 and 64.6 nm under SEM analysis and additional substantiated by XRD results. A hexagonal wurtzite shape observed for the synthesized AgNPs, and the particle sizes were in the order of 32.16–32.17 nm as reckoned by Debye-Scherer's formula. The elemental analysis has performed using EDS authenticated the silver content of 69.06 and 54.48 for RCR-AgNPs and RCS-AgNPs, which testifies the explicit biosynthesis of nanoparticles. Further, the AgNps showed vital antibacterial potency against *Escherichia coli, Bacillus subtilis, Staphylococcus aureus, and Pseudomonas aerogenes*. The biosynthesized nanoparticles were report as a great antibiofilm agent against *P. auriginosa* and *E. coli.* Besides, the nanoparticle showed low to moderate cytotoxicity activity against human blood cells shows, the use of RC silver nanoparticles. Outcomes assert that biosynthetic AgNPs produce an exceptional potential alternative to present-day chemical compounds.

Keywords: *Rubia cordifolia*, Antibacterial, Antibiofilm, Cytotoxicity.

QUICK RESPONSE CODE →

DOI: 10.47583/ijpsrr.2021.v67i02.028

DOI link: http://dx.doi.org/10.47583/ijpsrr.2021.v67i02.028

INTRODUCTION

Nanotechnology is one of the new frontier areas of chemistry that involves the study of the physical and chemical properties of the material at the nanoscale [1]. A larger surface area with high atomicity is the principal advantage of nanostructured materials. This unique property of nanomaterials was made applicable in both biology and industry [2].

Bio-nanotechnology, an integral part of nanotechnology, links the nanotechnology with biology. The synthesis of nanoparticles using biological samples tenders an environmentally sustainable approach in formulating the drug for pharmaceutical purposes [3]. In the biosynthesis of nanoparticles, the biodegradable polymer, plant extracts, and even microorganisms are being managed as reductants or capping agents in the bio-based synthesis of nanoparticles [4]. The main impediment in the synthesis of nanoparticles exercising microorganisms is that it requires the laborious and tedious workup schemes. Also, there are multiple unpropitious consequences entailed in the chemical synthesis of nanoparticles, such as practicing alkali solvent, inadvertent byproducts, and tiresome isolation modes. These detriments possibly subdued by adopting plant extracts in the green synthesis of Nanoparticles that requires much simple investigative and mild isolation procedures of nanoparticles [5.] Plants embrace diverse phytochemicals like ketones, aldehydes, terpenoids, flavones, amides, and carboxylic acids. The chemical compounds, when treated with metal ion solution, reduce them to Nanoparticles [6]. The biosynthetic nanoparticles extend copious benefits over chemically integrated ones [7]. Recently, the biosynthesis of nanoparticles has snagged the attention of researchers worldwide. As they include environmentally benign systems, and such nanoparticles confer exceptional stability along with the maintenance of biological importance [8].

Growing in multiple antibiotic resistances of pathogens has created great havoc to the human population. One of the possible mechanisms for the resistance by antibacterial drugs transpired possibly demonstrated by the formation

of biofilm. Biofilms are densely packed communities of microbial cells that grow on living or inert surfaces and surround themselves with secreted polymers like exopolysaccharides. Exopolysaccharide matrix or glycocalyx generation is a part of the distinguishing peculiarities of the biofilms. As purported, this matrix prevents the access of antibiotics to the bacterial cells embedded in the community in addition to other functions [9]. Researchers have concluded that biofilms are currently estimated to be responsible for over 65% of nosocomial contagions and 80% of all microbial epidemics [10]. For example, urinary tract (UTIs) infections and catheter diseases are responsible for persistence ailments causing relapses and acute prostatitis [11].

The nanoparticles can interact with blood either by direct contact by subcutaneous injection or by oral inhalation, because of the smaller size and larger surface area [12]. After the administration of nanoparticles within the system, they can reach the vital organs of the body via the bloodstream. Consequently, the knowledge related to the potential significance of delivered nanoparticles on haemolysis, platelet count, and the coagulation of the blood in humans is quite limited. Haemolysis is the destruction of red blood cells, which may cause anemia and sometimes renal failure, primary and secondary haemostasis [13].

Silver nanoparticles (AgNPs) remaining one of the most comprehensively considered of all other nanoparticles [14] that own exceptional attributes like good electrical conductivity, physicochemical stability, and antimicrobial efficacy with low toxicity [15]. Because of their broad antimicrobial spectrum together with greater efficacy against some bacteria, AgNPs have had extensively practiced in consumer products than any distinct nanomaterials, particularly in both consumer and biomedical applications. The biosynthesized silver nanoparticles using medicinal plants determine encouraging antimicrobial activity toward human pathogens [16]. The silver nanoparticles principally kill pathogens by rupturing the cell wall of pathogens and then altering the permeability of the cell wall followed by infringing the biochemical process, further enter deeply into the cell and interacts with DNA causing the cell death[17].

Rubia cordifolia (RC), a plant that is prominent in India as Manjishtha or Indian madder, belongs to the Rubiaceae family. Roots of RC was known for its effectiveness in treating Jaundice and diabetic foot ulcers, and its stem served to cure snake bites and scorpion sting. Numerous literature during the last few decades details the applications of distinct parts of RC in the therapy of various illnesses such as diabetes, cancer, Alzheimer's, and microbial infection. The plant also has been published as an analgesic, gastroprotective, immune modulator, and gastroprotective agents [18]. Because of its medicinal importance, green synthesis of AgNPs performed by utilizing the plant's stem and roots. Further, an attempt made to correlate the bioactive potential of stem and root mediated AgNPs.

MATERIALS AND METHODS

Preparation of sample and reagents

Collection of Rubia cordifolia (RC):

Rubia cordifolia root and stem were picked randomly from plants grown at the sericulture department, University of Mysuru, Mysuru. The stem and root were thoroughly washed in sterile distilled water for 10 min and then sundried for one day.

Preparation of water extracts of Rubia cordifolia Root and stem:

Fresh RC root and stems diced into small pieces; 10 g of fresh root and stem had located in a separate flask containing 50mL of distilled water and heated at 60 °C for 40 min. After heating, Rubia cordifolia root (RCR) and stem (RCS) extract were filtered and stored in an amber color bottle at 4 °C.

Biosynthesis of RCR-AgNPs and RCS-AgNPs from water extract of RCR and RCS:

10 mL of root and stem extracts were taken in a beaker and added 50 mL of 1 mM $AgNO_3$ solution slowly with consistent stirring at 60 °C. The change of color of the RCR extract from yellow to red intimated the synthesis of silver nanoparticles from the water extract of RCR & RCS by reduction. The content was centrifuged at 10,000 rpm for 20 min and practiced for further analysis. The extract was concentrated under vacuum at 45 °C to secure powder and stored at 4 °C for further characterization investigations. Besides, the same procedure has been maintained for the synthesis of RCS-AgNPs and characterized by managing different analytical tools.

Characterization

UV-Vis Spectrophotometer and Automatic microplate reader:

The reduction from Ag^+ to Ag^0 after adding 1 mM $AgNO_3$ solution to RC root and stem for the synthesis of RCR-AgNPs and RCS AgNPs monitored utilizing UV visible spectral analysis (Beckman-Coulter DU-730 UV-Vis Spectrophotometer, USA) with wavelength (λ) scan from 200 to 800 nm. The optical density (OD) of the biofilms were detected by automatic microplate reader (Genetix, Biotech Asia Pvt.Ltd).

Scanning Electron Microscope (SEM):

The powdered sample of RCR-AgNPs and RCS AgNPs placed on a carbon-coated plate and plate was gold-coated by a sputter-coating instrument to enhance the conductivity and accuracy of the picture. Scanning electron microscope (Hitachi, S-3400N, Japan) was used to analyze the morphology and size of produced RCR-AgNPs and RCS AgNPs.

Energy-Dispersive X-ray spectroscopy (EDS):

EDS (Thermo fisher scientific, Noran System 7, USA) analysis of *RCR-AgNPs* and RCS AgNPs carried out to examine the crystalline nature. Also, to observe the optical absorption of the peak from surface plasma response, other elemental O, Cl signals were registered to identify enzymes and other proteins existing in the integrated *RCR-AgNPs* and RCS AgNPs.

Fourier Transformed –Infra Red (FT-IR) Spectroscopy:

The functional groups present in the RC root and stem extract used in the synthesis of *RC-AgNPs* was validated by FTIR (PIKE Technologies, Spectrum Two, USA) at 4000-600 cm^{-1} range of wavelength.

X-ray diffraction studies:

The crystal structure identification confirmation for synthesized *RC-AgNPs* performed by powder XRD (RIGAKU X-ray diffractometer, model-smart lab 3 kW with Cu K_α source at 2ϑ angle probed 100-800). Fine powder of *RC-AgNPs* was placed in a plate and scanned to detect the width of XRD peaks at a rate of 3^o min^{-1}, and the average size of the *RC-AgNPs* was determined using de-Broglie equation ($n\lambda = 2d\sin\vartheta$).

Dynamic Light scattering (DLS):

Distribution of particle size and zeta potential of synthesized *RC-AgNPs* was detected performing DLS (Microtrac- DLS, W3231).

Determination of antimicrobial activity of green synthesized AgNPs from root and stem

Antibacterial activity

The zones of inhibition at variable concentrations of RC root and stem had screened for antibacterial as against both Gram-positive (*S. aureus* MTCC 7443*, B. Subtilis*) and Gram-negative (*E. coli* MTCC 7410, and P.*aeruginosa* MTCC 733) bacterial strains along with streptomycin were ventured by disc diffusion method [19]. The test bacteria disseminated uniformly over the cultured exterior of LB agar media, possessing a concentration of 1.5 x 108 CFU mL^{-1}, with a sterile glass spreader. The sterile discs (6 mm) were loaded with 50 µL of RCR-AgNPs, RCS-AgNPs (dispersed in sterilized distilled water), and placed on agar plates along with standard streptomycin. The inoculums made under PBS and incubated, the inoculated plates for 24 h at 37 ± 2°C, and measured the zone of inhibition around the discs. The experiment repeated in triplicates along with standard.

Minimum inhibitory concentration test (MIC)

The determination of MIC of silver nanoparticles did succeed by broth microdilution [20]. The stock solutions (100mg/mL) of biosynthetic RCR-AgNPs, RCS-AgNPs, and controls were prepared. About 100 µL of stock solution diluted two-fold serially, and were added individually (5-0.002 mg/mL). A 10 µL of inoculums suspension was added for each well and incubated at 37 ± 2 °C for 24 h. Absorbance was measured at 620 nm without agitation using ELISA plate reader (Lab Tech 4000). MIC was also confirmed by adding TTC (2, 3, 5-triphenyltetrazolium chloride) of 10 µL well (2 mg/mL) and incubated for 30 min. The minimum concentration at which no color change witnessed had taken as the MIC. The experiment repeated in triplicates along with standard.

Toxicity Test (Haemolytic activity)

As the AgNPs have excellent antimicrobial characteristics, due to their potential blood contact, the toxicity test performed under in-vitro conditions to get insights into the mechanisms for blood compatibility. Hemolysis, the rupture of erythrocytes (red blood cells), and the ouster of their contents (e.g., hemoglobin) into the surroundings, that produces anemia, jaundice, and renal malfunction. In this study, we have investigated hemolysis, of RCR-AgNPs, and RCS-AgNPs. These nanoparticles possess a large surface area, due to which a significant increase in in-vitro hemolysis had observed with AgNPs matched with micron-sized particles. Human erythrocytes accumulated from apparently healthy individuals, then the blood was centrifuged at 300 rpm for 10-15 minutes. A 2% erythrocyte suspension transpired in a sterile PBS for hemolytic study. Various concentrations of metal oxides prepared using 0.85% NaCl, and then 2% human erythrocyte suspension was added and then incubated at 37 °C for 1 hour. After incubation, the cells were pelleted at 5000 rpm for 10 minutes and determined the absorbance of the collected supernatant at 450 nm using a spectrometer. In the negative control, the only buffer was used for background lysis, whereas in positive control lysis, the buffer used for complete lysis of the erythrocytes. For each sample, the percentage of maximum hemolytic activity determined.

Biofilm inhibition assay

The ability of the biofilm formation inhibition by AgNps was investigated by Microtiter plate (MtP) assay. Different concentrations (100%, 50%, 25%, and 12.5%) of Ag NPs were prepared by suspending the nanoparticles in double-distilled water. Individual wells of sterile, polystyrene, 96 well-flat bottom tissue culture plates (TCP) were filled with 180 µL of BHI broth and inoculated with 10 µl of overnight culture (OD 620=0.01). After vigorous vortex mixing, 10 µL of AgNPs were added immediately from the stocks to the wells. The final volume in every well was 200 µl. The tissue culture plates were incubated for 24 h at 37 ºC. Subsequently, the content of each well removed gently. The wells were washed four times with phosphate-buffered saline solution (pH = 7- 7.2) to remove free-floating planktonic bacteria. The biofilms formed by bacteria were fixed in ethanol (95%) and stained with crystal violet (0.1%, w/v) for 20 min. The excess stain was rinsed off by several times washing with deionized water and kept the plates for drying. 200 µL of glacial acetic acid (33%) added to each well, and after 15 minutes, the optical densities (OD) of the stained adherent bacteria, determined spectrophotometrically at 590 nm by a

microplate reader. The OD values have treated as an index of bacteria adhering to the surface of biofilms. The studies had duplicated in triplicates.

RESULTS AND DISCUSSION

Characterization of biosynthesized AgNPs

UV-Vis spectroscopy and DLS Analysis of Biosynthesized Nanoparticles

The efficiency of the green biosynthesis process of AgNPs was performed by using a UV-vis spectrophotometer in the range from 200-800 nm. In this study, an intense absorption peak observed in the range of 242 and 243 nm for RCR-AgNPs and RCS-AgNPs individually (Figure. 1). It is evident from reports published elsewhere that AgNPs exhibit UV-visible absorption spectra in the range of 200-350 nm [21]. Therefore, the presence of a characteristic sharp and distinct peak displayed at 242 and 243 nm substantiates the biosynthesis of AgNPs. And no such peculiar peak was found in the control set purporting no reduction of Ag+ ions. The reduction process of silver ions and the biosynthesis of stable AgNPs transpired within 24 hours of reaction.

A

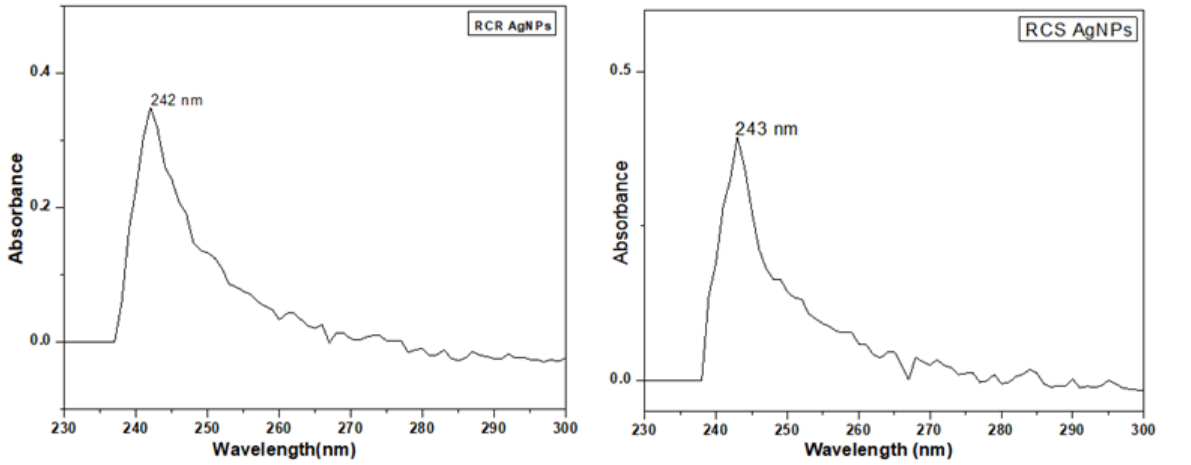

B.

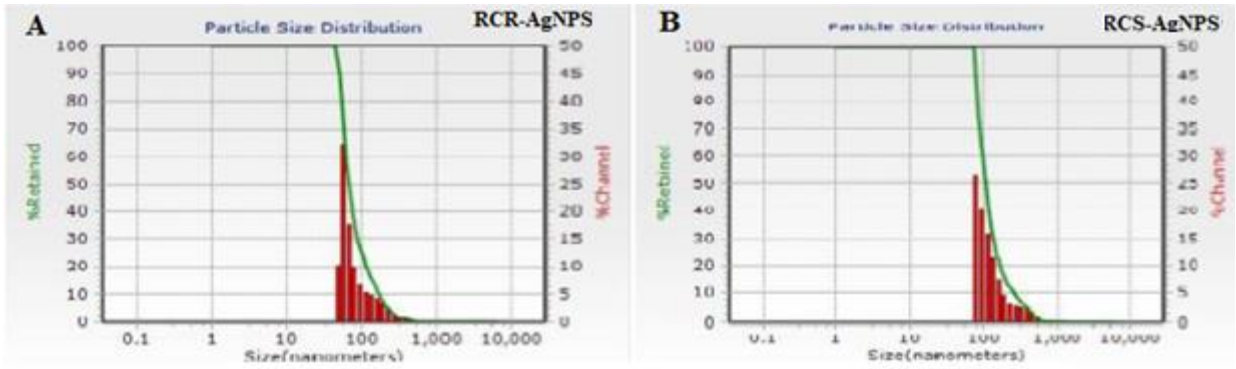

Figure 1: Showing UV-vis spectra of the biosynthesized RCR-AgNPs and RCS-AgNPs (A), and Dynamic light scattering (DLS) analysis of Nanoparticles (B)

DLS analysis is one of the reliable techniques for the characterization of nanoparticles in the solution for particle size distribution and zeta potential as well [22]. The histogram of DLS analysis for the particle size distribution of RCR-AgNPs and RCS-AgNPs has shown in Fig. 2. Fig. 2 manifested the details of the peak summary of RCR-AgNPs and RCS-AgNPs. The interplay of biosynthesized nanoparticles with the biological systems was determined by the surface charge distribution or zeta potential and found to be -147.5 and -147.1 mV individually, for RCR-AgNPs and RCS-AgNPs. The zeta potential with -10 and + 10 mV indicates that the Nps have a neutral charge, however with a value above +0.32 fC and +2.98 fC, considered to be cationic and anionic, sequentially [23]. Moreover, the biosynthesized RCR-AgNPs and RCS-AgNPs confer an average diameter of 64.6 nm and 105 nm, each, in the aqueous colloidal solution.

X-ray Diffraction (XRD) analysis:

The crystalline nature of the biosynthesized RCR-AgNPs and RCS-AgNPs had evaluated by the X-ray diffraction (XRD) technique and used to assess the average size, bravais lattice, and surface structure of nanoparticles [24]. The XRD patterns indicating the sharp peaks for RCR-AgNPs and RCS-AgNPs visualized in Fig. 3a and 3b (mark in the diagram) sequentially. The diffractogram of RCR-AgNPs & and RCS-AgNPs showed well-resolved three diffraction peaks at 2θ angles of 27.98°, 32.48° and 38.22° which correspond to the Braggs reflection peaks of (011), (000) and (001), of RCS-

AgNPs, respectively corresponding to hexagonal wurtzite (PDF Card No.: 01-071-5209 Quality: I). Further, the average crystal size (d) of biosynthesized AgNPs established by adopting the Debye-Scherrer formula:

$$d = k\lambda / \beta\cos\theta$$

Where k is the crystallite-shape factor with value 0.9, λ is the wavelength of the X-rays from Cu Kα radiation source (1.54 Å), ϑ corresponds to the Bragg angle, and width (full-width at half-maximum) of the X-ray diffraction peak in radians, and β is the full width at half maximum (FWHM) of the planes at the diffraction angle ϑ [25]. The figured average crystallite size was determined to be 221.16 nm and 219.62 nm for RCR-AgNPs and RCS-AgNPs sequentially.

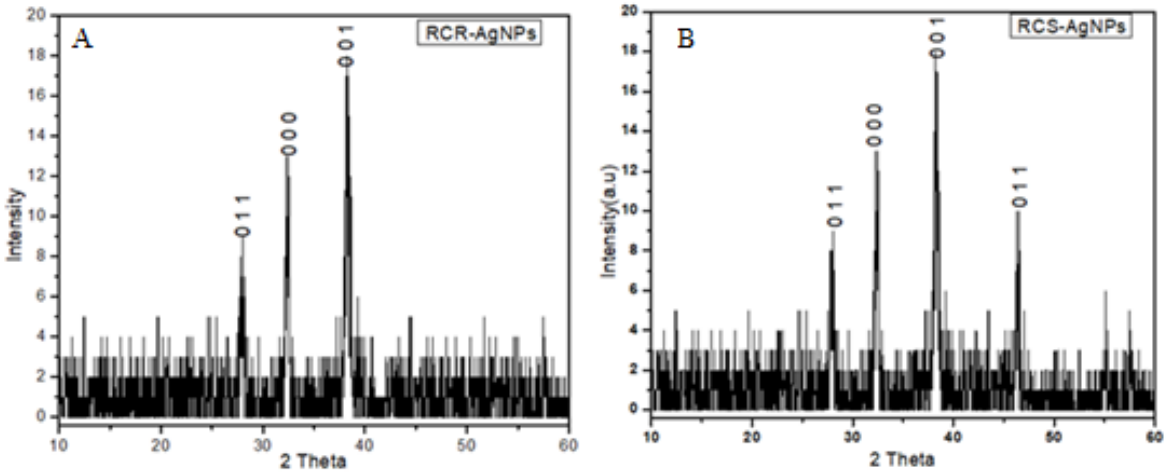

Figure 2: X-ray spectra of RCR-AgNPs and RCS-AgNPs

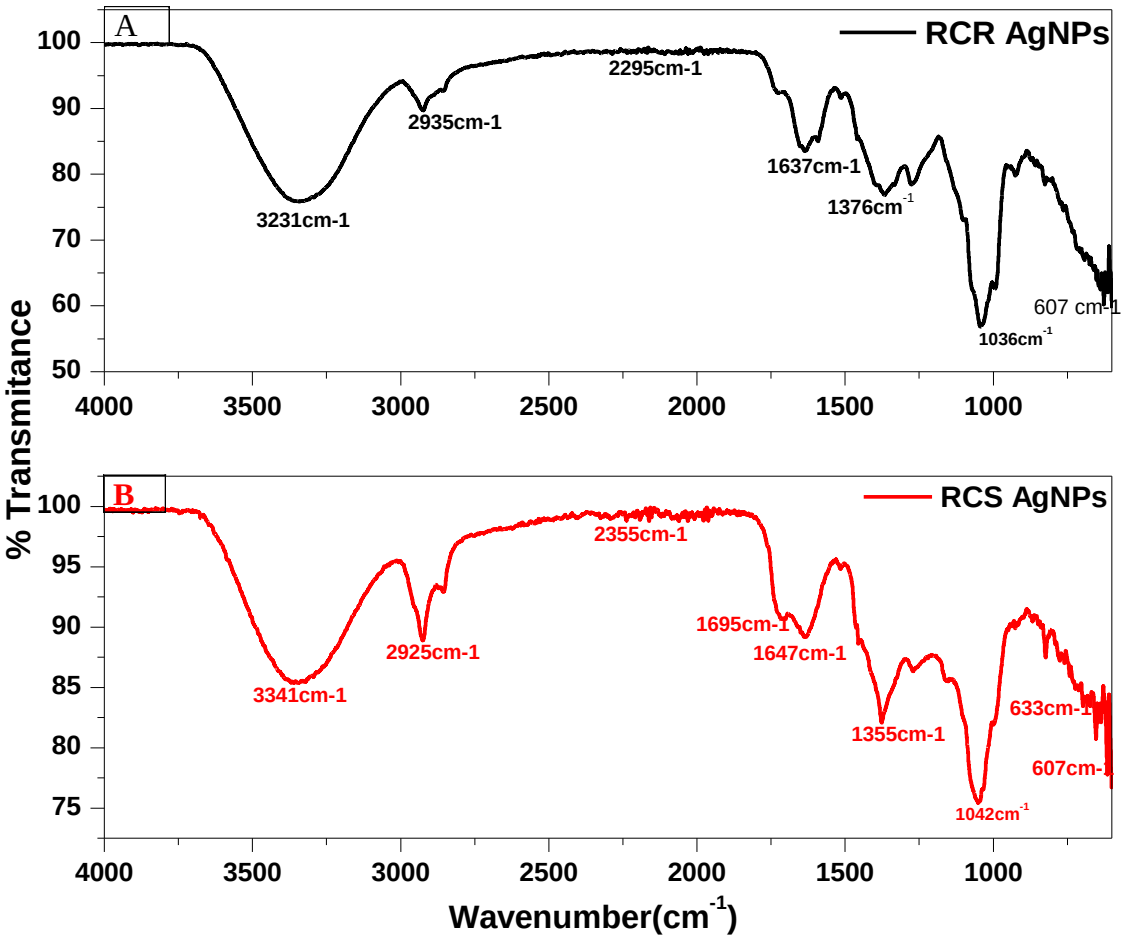

Figure 3: FTIR spectra of biosynthesized TTL-AgNPs (A) and TTF-AgNPs.

Fourier Transformed –Infra Red (FT-IR) Spectroscopy:

The FT-IR spectroscopic analysis was probed to surmise the information on the plausible biomolecules of RC liable for the integration of RCR-AgNPs and RCS-AgNPs represented as Fig.4A and B sequentially. The analysis of the FT-IR spectrum of plant extracts of RCS-AgNPs characterized by the sharp peak observed at 1637cm^{-1}, and 801 cm^{-1}, which corresponds to carbonyl stretching frequency[26] and CH phase bending individually. The band at 1364 cm^{-1} and 2920 cm^{-1} representing the carboxylic group and NH stretching frequency, a band observed at 3341 cm^{-1} related to the hydroxyl group[27].

Similarly, the FTIR analysis of RCS-AgNPs (Fig. 4B), indicated a sharp peak recognized at 1638.5cm^{-1} corresponding to CO stretching[28]. The bands observed at 607 and 633cm-1 symbolizing the Nitrogen-containing bio ligands[29]. The bands noticed at 802cm^{-1}, 1376.49cm^{-1}, and 2925 cm^{-1} corresponds to aromatic CH bending, the carboxylic group, and NH stretching frequency. Moreover, another band at 3231cm^{-1} of about the O-H group bonded [30]. By matching the FTIR spectra of RCR-AgNPs and RCS-AgNPs, a typical peak positioned at 3346 cm^{-1} complies with OH stretching. For both the specimens, the CO stretching resembles in the region of 1637.33 and 1638.5cm^{-131}. From the spectra, it is evident that the O-H and C=O groups were adsorbed on the exterior of AgNPs and implicated in the reduction process.

SEM and EDS analysis:

The surface morphology of biosynthesized RCR-AgNPs and RCS-AgNPs had scrutinized with SEM. Evidently, from the SEM photograph of the RCR-AgNPs and RCS-AgNPs sample, discerned the morphology of the particles was almost hexagonal shape[32] and, slightly agglomerated attributable to the interplay within AgNPs. As can be witnessed that the AgNPs grains are spaced uniformly throughout the surface, and therefore confirming the formation of nano-size crystallites (Figure 5). Further, the average grain size of RCR-AgNPs and RCS-AgNPs, calculated from the linear intercept method did found to be 64.6 and 105 nm, individually. The energy dispersive X-ray spectrometer was employed to discover the elemental analysis in chemical composition among the spherical architecture [33].

A

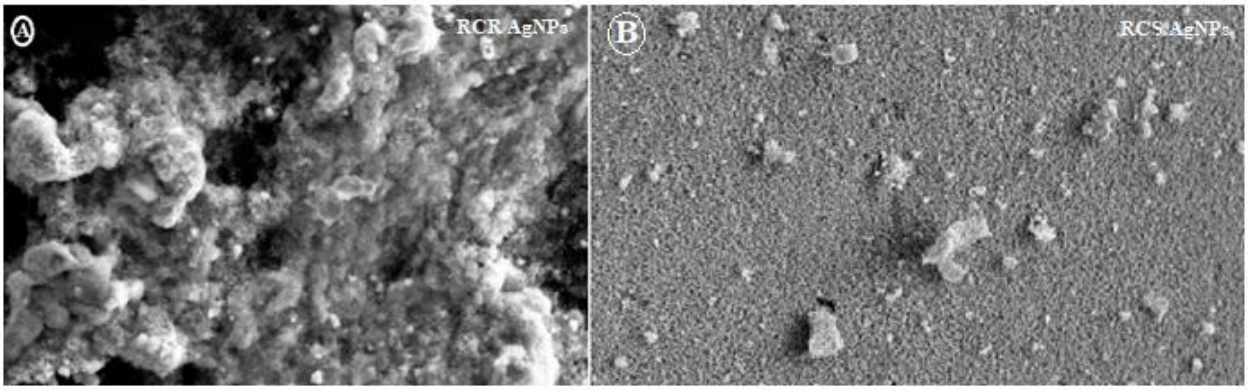

B

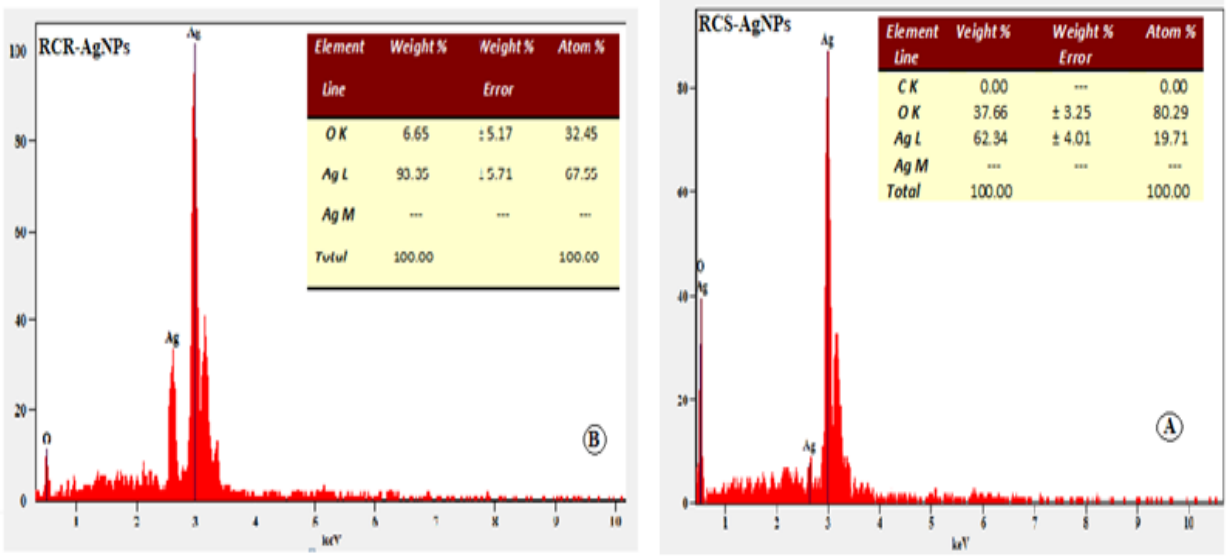

Figure 4: Showing SEM images and EDS analysis of synthesized RCR-AgNPs and RCS-AgNPs of *R. cordifolia*

Further insight into the structural features of RCR-AgNPs and RCS-AgNPs were analyzed quantitatively (Weight %) by EDS (Energy Dispersive Spectroscopy**)**, which showed the presence of pure AgNPs (Figure. 6). The EDS spectrum of RCR-AgNPs showed that the two peaks that recognized as silver (93.35%) oxygen (6.65 %). Furthermore, the elements of carbon and nitrogen had found in nanocomposites. Similarly, in RCS-AgNPs showed two peaks identified as silver (62.34 %) and oxygen (37.66 %), which also proves its purity.

Biological activity

In Vitro Antimicrobial activity of bio-fabricated AgNPs

The antibacterial activity of developed RCR and RCS extracts was evaluated against Gram-positive *S. aureus, B.subtilis, and* Gram-negative bacteria *P.aeruginosa, E.coli,* by standard disc diffusion method and the plates maintained using LB agar medium has shown in Fig 7. The widths of the zones of inhibition measured, and the mean value for a distinct organism was registered and denoted in millimeters. The diameter of the zone of inhibition (mm) around each containing AgNPs generated exposed in Fig 8. It concluded that, among the test bacteria, susceptibility was noted maximum in the case of *E. coli*, and *B. Subtilis* conferred immense antibacterial activity for RCRAgNPs (8.2 and 6.2 mm). Whereas, the RCSAgNPs have determined the activity of 5.2 and 5.3 mm. But, the inhibition of test bacteria by standard antibiotics was higher (6.6mm) when compared to RCSNPs (4.1mm) extracts. Whereas the *S. aureus,and P.aeruginosa* have shown lesser activity for **RCS AgNPs** (5.3 and 4.3 mm) in comparison with standard. The reference antibiotic-induced enhanced inhibition in all the strains, and there was no inhibition for the blank alone. Therefore the RCRAgNPs showed good antibacterial activity for gram-positive bacteria in comparison with the standard.

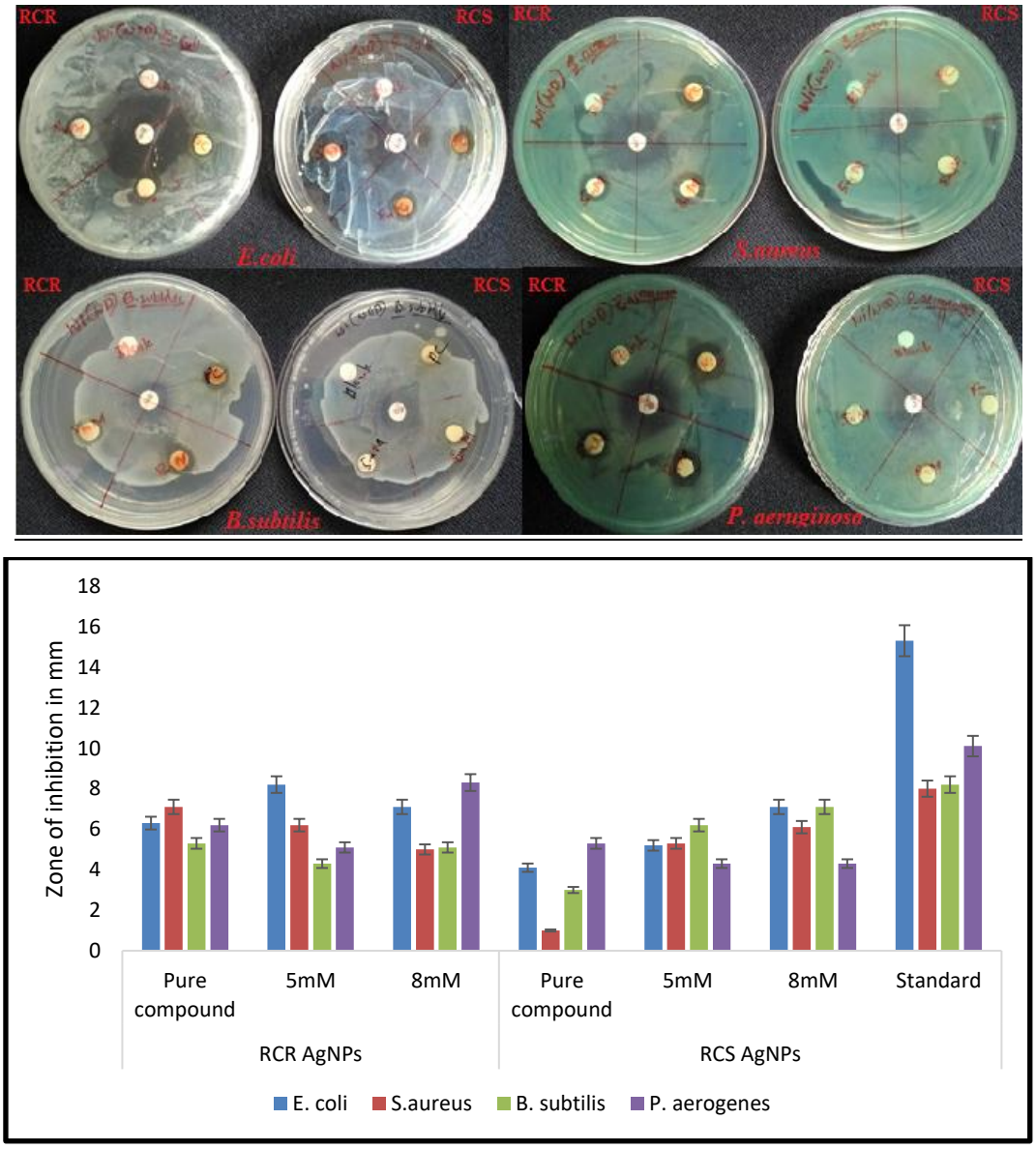

Figure 5: The antimicrobial activity of Biosynthesized nanoparticles against *Escherichia coli, Bacillus subtilis, Staphylococcus aureus, and Pseudomonas aerogenes* by disk diffusion method

Minimum Inhibitory Concentration (MIC) by Microliter Broth Dilution Method

The MIC values for both RCR AgNPs and RCS AgNPs extract against the bacterial strains- *Escherichia coli*, Pseudomonas aeruginosa, *Staphylococcus aureus* and B. Subtilis determined by the serial dilution method. 10^{-6} cfu/mL bacterial culture used, the concentration of RCR, RCS, RCR AgNPs, and RCS AgNPs used in this measurement was about 2-8 mM. Furthermore, the MIC values of RCR are 10^{-7}, 10^{-9}, and 10^{-6} for 2, 5, and 8 mM individually, whereas, for RCR AgNPs are 10-5 for both 2 and 5 mM and 10^{-7} for 8 mM concentration. While the MIC values of 4.893 and 10.5 in *E-coli*. RCS AgNps is 10^{-7}, 10^{-9}, and 10^{-6} for 2, 5, and 8 mM concentrations sequentially for E.coli was 13.764, 6.104 and 12.965 respectively. On the other hand, for *S. aureus* the MIC value of RCR and RCS AgNPs evaluated to be 10^{-4}, 10^{-5} was for 2, 5, and 8 mM concentrations were 12.96 and 23.28, RCS was 1.51, 3.250 respectively. *B.subtilis* was found to be 10^{-3},10^{-6} and 10^{-8} for (32.538, 17.529, 13.97 and RCS was 1.823,1.678,15.79) 2mM, 5mM and 8mM correspondingly. *P.aeruginosa* was evaluated to be 10^{-7}, 10^{-4} for 2, 5m and 8mM concentration. For RCRAgNPs 42.946, 10.48 and RCS AgNPs was 10.067, 1.972 respectively. Among the analyzed four strains, *s.aureus* was most sensitive with the least MIC values [34].

Toxicity Test (Hemolytic Activity)

The toxicity of AgNPs had checked by hemolysis. Hemolysis occurs when the red blood cells come in abutment with water and essential to consider this imbed essence prior to use. As well tabulated that the appropriate limit of hemolysis for biomedical substances requires under 5% in all the cases [35]. The Hemolysis percentage of ACD blood with RCR AgNPs and RCSAgNPs found to be 0.082 and 0.874 % correspondingly. And importantly, both the AgNP's offered very less hemolysis (1.7%), purporting their inferior toxicity. RCS and RCR silver nanoparticles showed dose dependent percentage of lysis in RBC cells. Highest concentration of RCR silver nanoparticles showed lower hemolysis, i.e RCR is not toxic to cells compared to RCS. Whereas, RCR lowest concentration 12.5 % (0.082), 25 (1.088), and 50% (1.911) and RCS was lowest concentration of 12.5 % (0.874), 25 % (0.344), and 50% (1.577) indicated the percentage of hemolysis was 1% but highest concentration of the RCR was below 1%. Its indicating that RCR silver nanoparticles are less toxic compared to RCS.

***In vitro* antibiofilm assay**

Prevention of cell attachment: antibiofilm activity/ anti-adhesion

The effect of RCR and RCS AgNPs on the attachment and inhibition of biofilm formation is given in Fig.10. The percentage inhibition values between 0 to 100% signify inhibition of biofilm, while enhancement of growth is reflected by values below 0%. Above the 50% inhibition marks the activity is regarded as good, while it is poor if it is between 0 and 49%. The plant extracts had varying degrees of activity on the prevention of attachment. Four of the extracts had good prevention of biofilm attachment against *E. coli* (> 50%), three extracts had inhibition less than 50% while the extracts of RCR AgNPs and RCS AgNPs enhanced the biofilm growth and hence were not included in the biofilm development assay. Both RCR and RCS AgNPs prevented attachment of *P.aeruginosa* with values above 50%. Extracts evaluated against *E. Coli* prevented cell attachment while *P. aeruginosa and E.coli* A enhanced biofilm attachment and growth [36].

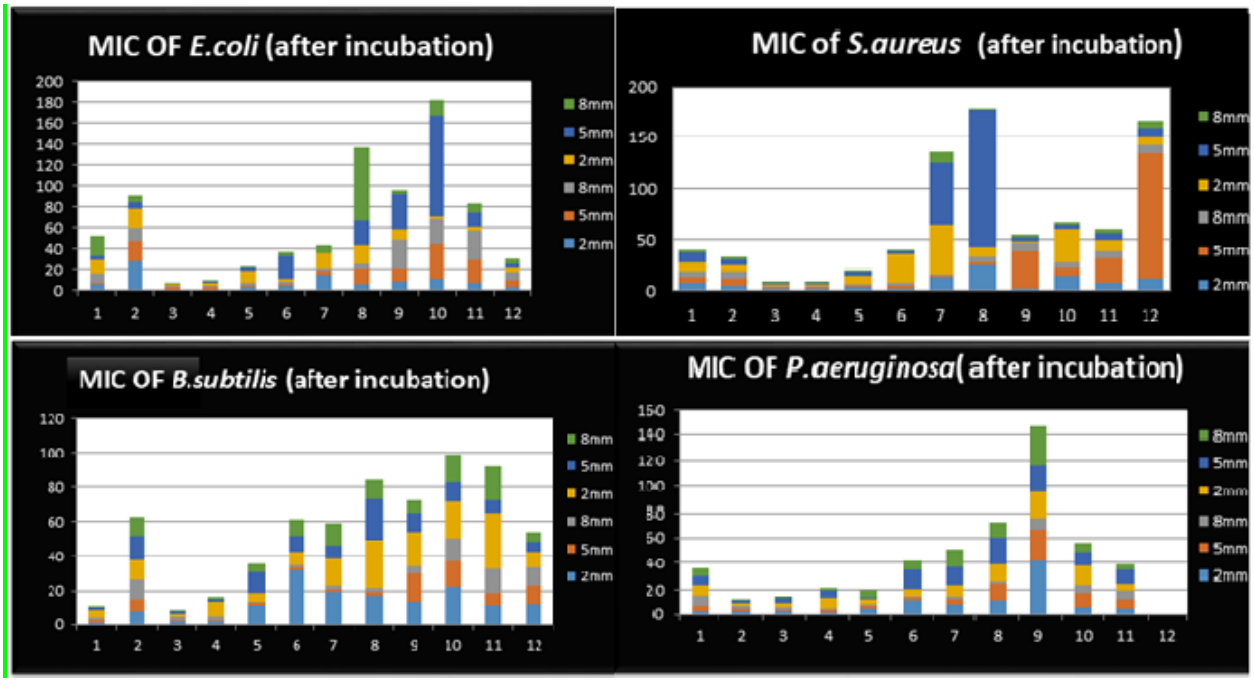

Figure 6: Minimum Inhibitory concentration analysis of biosynthesized nanoparticle against

A

B

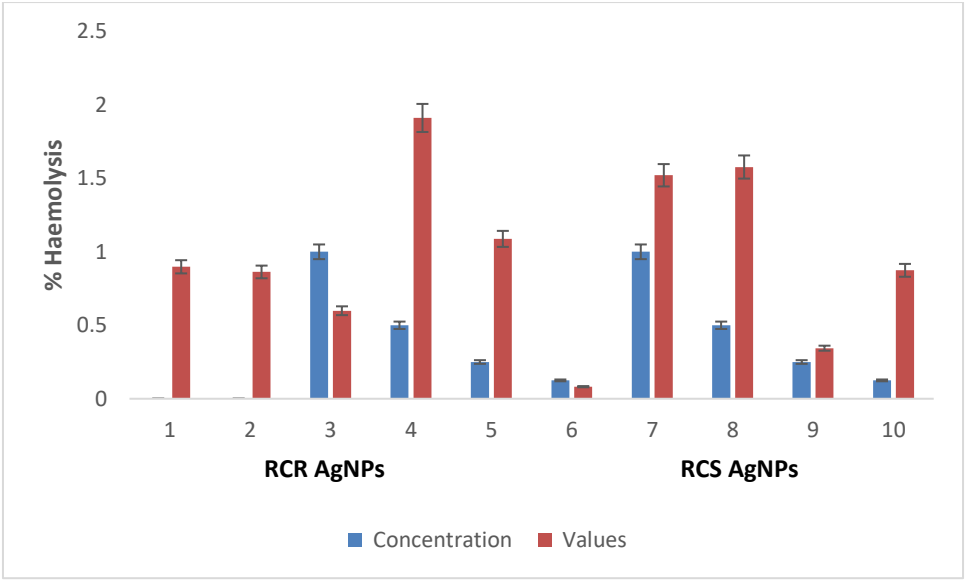

Figure 7: Cytotoxicity analysis of the biosynthesized nanoparticles using RBC cells by Hemolytic analysis

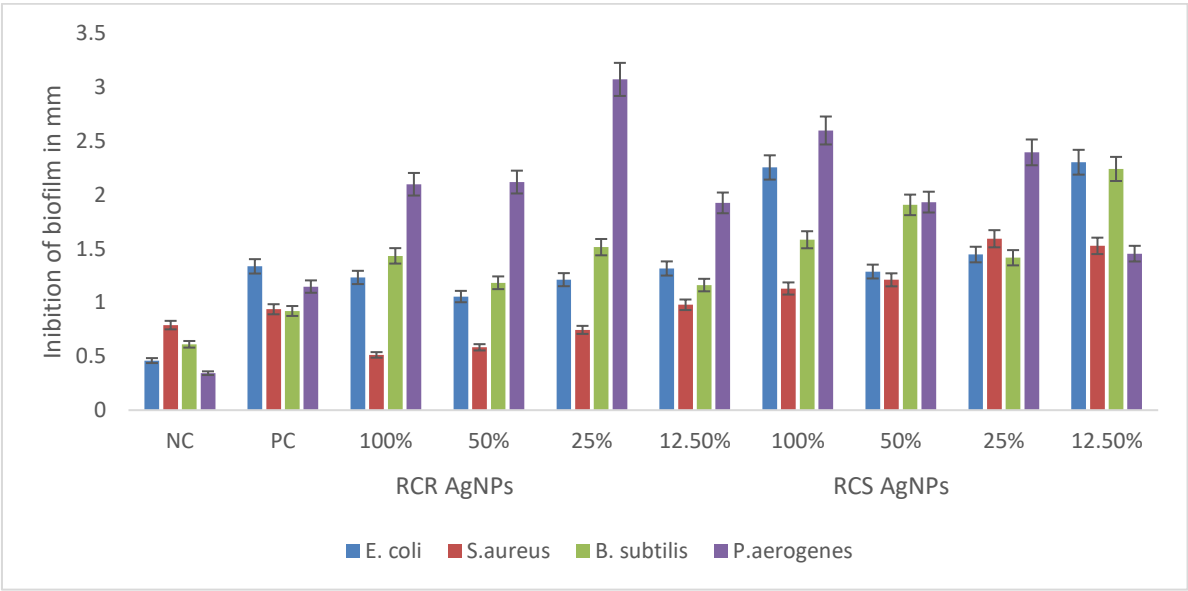

Figure 8: Graphical representation of inhibition of Biofilm formation by different concentrations of RCR and RCS AgNPs on biofilm formation of P. aeruginosa and *E.coli* tested bacteria with the positive and negative control according to OD values after 24 h of incubation**.**

CONCLUSION

In this exploration, aqueous extracts of root and stem of *R. cordifolia* was successfully used for green synthesis of silver nanoparticles. Characterization of the synthesized silver nanoparticles, performed by using various physicochemical routines like UV-vis spectroscopy, DLS, XRD, FT-IR, and SEM-EDS. The UV-vis spectral analysis explicates the absorption at 242 and 243 nm, which is a characteristic peak for Silver nanoparticles. The DLS and XRD analysis affirmed that the particle size is in the order of 65 and 68 nm to RCR-AgNPs and RCS-AgNPs correspondingly. The FT-IR spectroscopy witnessed the existence of appropriate functional groups of the plant component formed a complex with silver oxide. The morphological considerations of the bio-fabricated AgNPs carried out by SEM analysis revealed the agglomerated nanoparticles cause significantly less hemolytic toxicity. The 100% purity of these AgNPs confirmed by EDS and the biosynthesized AgNPs bestowed better antimicrobial efficacy. The proceeds from the above spectral examinations verify that the biosynthesized AgNPs from *R. cordifolia*, a significant contribution too many biological applications such as antimicrobial, hemolytic, and biofilm assay. Furthermore, the specific biological applicability of this bio fabricated AgNPs is under progress.

Acknowledgments: The authors gratefully acknowledge Clarette biotech pvt ltd, Mysore, CPEPA, vijnana bhavan, university of Mysuru, Mysuru, VVIT Research center Mysore and the authors also grateful to the Management of JSS Mahavidyapeetha, Mysuru, and Principal, JSSATE, Bengaluru for the facilities and encouragement.

REFERENCES

1. Jeevanandam J, Barhoum A, Chan YS, Dufresne A, Danquah MK. Review on nanoparticles and nanostructured materials: history, sources, toxicity and regulations. Beilstein journal of nanotechnology. 2018 Apr 3;9(1):1050-74. https://doi.org/10.3762/bjnano.9.98.
2. Forough M, FAHADI K. Biological and green synthesis of silver nanoparticles. Turkish journal of engineering and environmental sciences. 2011 Feb 28;34(4):281-7. https://doi.org/10.3906/muh-1005-30.
3. Das RK, Pachapur VL, Lonappan L, Naghdi M, Pulicharla R, Maiti S, Cledon M, Dalila LM, Sarma SJ, Brar SK. Biological synthesis of metallic nanoparticles: plants, animals and microbial aspects. Nanotechnology for Environmental Engineering. 2017 Dec;2(1):1-21. https://doi.org/10.1007/s41204-017-0029-4.
4. Ikram S. Synthesis of gold nanoparticles using plant extract: an overview. Nano Research. 2015;1(1):5.
5. Aljabali AA, Akkam Y, Al Zoubi MS, Al-Batayneh KM, Al-Trad B, Abo Alrob O, Alkilany AM, Benamara M, Evans DJ. Synthesis of gold nanoparticles using leaf extract of Ziziphus zizyphus and their antimicrobial activity. Nanomaterials. 2018 Mar;8(3):174. https://doi.org/10.3390/nano8030174.
6. Singh J, Dutta T, Kim KH, Rawat M, Samddar P, Kumar P. 'Green'synthesis of metals and their oxide nanoparticles: applications for environmental remediation. Journal of nanobiotechnology. 2018 Dec;16(1):1-24. https://doi.org/10.1186/s12951-018-0408-4.
7. Pantidos N, Horsfall LE. Biological synthesis of metallic nanoparticles by bacteria, fungi and plants. Journal of Nanomedicine & Nanotechnology. 2014 Sep 1;5(5):1. https://doi.org/10.4172/2157-7439.1000233.
8. Abou El-Nour KM, Eftaiha AA, Al-Warthan A, Ammar RA. Synthesis and applications of silver nanoparticles. Arabian journal of chemistry. 2010 Jul 1;3(3):135-40. https://doi.org/10.1016/j.arabjc.2010.04.008.
9. Prestinaci F, Pezzotti P, Pantosti A. Antimicrobial resistance: a global multifaceted phenomenon. Pathogens and global health. 2015 Oct 3;109(7):309-18. https://doi.org/10.1179/2047773215Y.0000000030.
10. Famuyide IM, Aro AO, Fasina FO, Eloff JN, McGaw LJ. Antibacterial and antibiofilm activity of acetone leaf extracts of nine under-investigated south African Eugenia and Syzygium (Myrtaceae) species and their selectivity indices. BMC complementary and alternative medicine. 2019 Dec;19(1):1-3. https://doi.org/10.1186/s12906-019-2547-z.
11. Choccalingam C. Volume, conductance, and scatter parameters of neoplastic and nonneoplastic lymphocytes using Coulter LH780. Journal of laboratory physicians. 2018 Jan;10(1):85. https://doi.org/10.4103/JLP.JLP.
12. Laloy J, Minet V, Alpan L, Mullier F, Beken S, Toussaint O, Lucas S, Dogné JM. Impact of silver nanoparticles on haemolysis, platelet function and coagulation. Nanobiomedicine. 2014 Sep 29;1:4. https://doi.org/10.5772/59346.
13. Namita P, Mukesh R. Medicinal plants used as antimicrobial agents: a review. Int Res J Pharm. 2012;3(1):31-40.
14. Rauwel P, Küünal S, Ferdov S, Rauwel E. A review on the green synthesis of silver nanoparticles and their morphologies studied via TEM. Advances in Materials Science and Engineering. 2015 Jan 1;2015. https://doi.org/10.1155/2015/682749.
15. Zhang XF, Liu ZG, Shen W, Gurunathan S. Silver nanoparticles: synthesis, characterization, properties, applications, and therapeutic approaches. International journal of molecular sciences. 2016 Sep;17(9):1534. https://doi.org/10.3390/ijms17091534.
16. Ponarulselvam S, Panneerselvam C, Murugan K, Aarthi N, Kalimuthu K, Thangamani S. Synthesis of silver nanoparticles using leaves of Catharanthus roseus Linn. G. Don and their antiplasmodial activities. Asian Pacific journal of tropical biomedicine. 2012 Jul 1;2(7):574-80. https://doi.org/10.1016/S2221-1691(12)60100-2.
17. Reidy B, Haase A, Luch A, Dawson KA, Lynch I. Mechanisms of silver nanoparticle release, transformation and toxicity: a critical review of current knowledge and recommendations for future studies and applications. Materials. 2013 Jun;6(6):2295-350. https://doi.org/10.3390/ma6062295.
18. Zsembik BA. Health issues in Latino families and households. Handbook of families & health: Interdisciplinary perspectives. 2005:40-61. https://doi.org/10.4135/9781452231631.n3.
19. Bachir RG, Benali M. Antibacterial activity of the essential oils from the leaves of Eucalyptus globulus against Escherichia coli and Staphylococcus aureus. Asian Pacific journal of tropical biomedicine. 2012 Sep 1;2(9):739-42.

https://doi.org/10.1016/S2221-1691(12)60220-2.

20. Rodriguez-Tudela JL, Barchiesi F, Bille J, Chryssanthou E, Cuenca-Estrella M, Denning D, Donnelly JP, Dupont B, Fegeler W, Moore C, Richardson M. Method for the determination of minimum inhibitory concentration (MIC) by broth dilution of fermentative yeasts. Clinical Microbiology and Infection. 2003 Aug 1;9(8): 1-8. https://doi.org/10.1046/j.1469-0691.2003.00789.x.

21. Anandalakshmi K, Venugobal J, Ramasamy V. Characterization of silver nanoparticles by green synthesis method using Pedalium murex leaf extract and their antibacterial activity. Applied Nanoscience. 2016 Mar 1;6(3):399-408. https://doi.org/10.1007/s13204-015-0449-z.

22. Maguire CM, Rösslein M, Wick P, Prina-Mello A. Characterisation of particles in solution–a perspective on light scattering and comparative technologies. Science and technology of advanced materials. 2018 Dec 31;19(1):732-45. https://doi.org/10.1080/14686996.2018.1517587.

23. Tomaszewska E, Soliwoda K, Kadziola K, Tkacz-Szczesna B, Celichowski G, Cichomski M, Szmaja W, Grobelny J. Detection limits of DLS and UV-Vis spectroscopy in characterization of polydisperse nanoparticles colloids. Journal of Nanomaterials. 2013 Jun;2013. https://doi.org/10.1155/2013/313081.

24. Bajpayee KK. Antifungal activities of bark extract of Calotropis procera (Ait.) R. Br. International Journal of Advances in Scientific research. 2015;1(02):108-10. https://doi.org/10.7439/ijasr.

25. Sharma R, Bisen DP, Shukla U, Sharma BG. X-ray diffraction: a powerful method of characterizing nanomaterials. Recent research in science and technology. 2012 Oct 19;4(8).

26. Narayanan KB, Sakthivel N. Green synthesis of biogenic metal nanoparticles by terrestrial and aquatic phototrophic and heterotrophic eukaryotes and biocompatible agents. Advances in colloid and interface science. 2011 Dec 12;169(2):59-79. https://doi.org/10.1016/j.cis.2011.08.004.

27. Mccash EM, Parker SF, Pritchard J, Chesters MA. The adsorption of atomic hydrogen on Cu (111) investigated by reflection-absorption infrared spectroscopy, electron energy loss spectroscopy and low energy electron diffraction. Surface Science. 1989 May 3;215(3):363-77. https://doi.org/10.1016/0039-6028(89)90266-5.

28. Kulkarni DR, Deshpande MN. Transition Metal Chelates of 2-[(2, 6-dichlorophenyl)-amino] Benzene Acetic Acid: Synthesis, Spectral Characterization and Antimicrobial Studies. Oriental Journal of Chemistry. 2012;28(4):1735-42. https://doi.org/10.13005/ojc/280424.

29. Krithiga N, Rajalakshmi A, Jayachitra A. Green synthesis of silver nanoparticles using leaf extracts of Clitoria ternatea and Solanum nigrum and study of its antibacterial effect against common nosocomial pathogens. Journal of Nanoscience. 2015;2015. https://doi.org/http://dx.doi.org/10.1155/2015/928204.

30. Nathiya A, Saleem H, Jayakumar T, Rajavel A, Babu NR. Molecular Structure and Vibrational Analysis of 2-(4-methoxyphenyl)-2, 3-dihydro-1h-perimidine Using Density Functional Theory. Journal of New Developments in Chemistry. 2017 Apr 26;1(2):70. https://doi.org/10.14302/issn.2377-2549.jndc-17-1488.

31. Hübner W, Mantsch HH. Orientation of specifically 13C= O labeled phosphatidylcholine multilayers from polarized attenuated total reflection FT-IR spectroscopy. Biophysical journal. 1991 Jun 1;59(6):1261-72. https://doi.org/10.1016/S0006-3495(91)82341-4.

32. Alaqad K, Saleh TA. Gold and silver nanoparticles: synthesis methods, characterization routes and applications towards drugs. J. Environ. Anal. Toxicol. 2016;6(4):525-2161. https://doi.org/10.4172/2161-0525.1000384.

33. Madasamy S, Liu D, Lundry J, Alderete B, Kong R, Robinson JP, Wu AH, Amento EP. Differential effects of lipid-lowering drugs in modulating morphology of cholesterol particles. JoVE (Journal of Visualized Experiments). 2017 Nov 10(129):e56596. https://doi.org/10.3791/56596.

34. Punjabi K, Mehta S, Chavan R, Chitalia V, Deogharkar D, Deshpande S. Efficiency of biosynthesized silver and zinc nanoparticles against multi-drug resistant pathogens. Frontiers in microbiology. 2018 Sep 20;9:2207. https://doi.org/10.3389/fmicb.2018.02207

35. Gondwal M, Joshi nee Pant G. Synthesis and catalytic and biological activities of silver and copper nanoparticles using Cassia occidentalis. International journal of biomaterials. 2018 May 2;2018.

36. https://doi.org/10.1155/2018/6735426.

37. Famuyide IM, Aro AO, Fasina FO, Eloff JN, McGaw LJ. Antibacterial and antibiofilm activity of acetone leaf extracts of nine under-investigated south African Eugenia and Syzygium (Myrtaceae) species and their selectivity indices. BMC complementary and alternative medicine. 2019 Dec;19(1):1-3. https://doi.org/10.1186/s12906-019-2547-z.

Source of Support: None declared.

Conflict of Interest: None declared.